SIMULATION-BASED DESIGN OPTIMIZATION OF LARGE-SCALE SEASONAL THERMAL ENERGY STORAGE IN RENEWABLES-BASED DISTRICT HEATING SYSTEMS

Abdulrahman Dahash, Fabian Ochs and Alice Tosatto
Unit of Energy Efficient Buildings, Department of Structural Engineering and Material
Sciences, University of Innsbruck, Innsbruck, Austria

ABSTRACT

A key lever to overcome the challenges in the buildings sector related to today's extensive utilization of fossil fuels is the introduction of renewables-based district heating systems. Thus, large-scale seasonal thermal energy storage (STES) systems found its place favorably in these systems. Yet, STES systems require a thorough planning to avoid the high investment. Consequently, numerical models gain importance as an alternative.

This work develops and validates an equation-based object-oriented tank model. Then, the work examines the influence of TES aspect ratio on performance and stratification. Then, the work inspects the insulation thickness impact on performance and cost.

INTRODUCTION

A key lever to the decarbonization of cities and districts is the systematic transition from the conventional based heating scheme into more sustainable one. Accordingly, the substitution of fossil fuels (e.g. natural gas) with renewable energy resources (e.g. solar energy, waste heat, geothermal energy) is investable and required.

Alongside this transition, district heating (DH) is seen as a key solution to relieve the energy problems in the heating sector, especially the concept of centralized heat production leading to efficient utilization of energy resources. Further, local available renewables are also introduced in this scheme forming renewables-based district heating (R-DH) systems.

To achieve a successful transition, it is of high importance to eliminate shortfalls in the renewables. Among all, the intermittency observed in renewables is the main frontier holding the full transition into renewable-based systems due to the fluctuating patterns (e.g. daily and seasonally) of renewables leading to risks such as the violation of security of supply.

Therefore, large-scale seasonal thermal energy storage (STES) systems are increasingly introduced in R-DH systems in order to capture the excess heat (e.g. industrial waste heat). By this virtue, large-scale TES makes heat available later when and where demand is observed. Yet, it is challenging to integrate STES units into R-DH system without ensuring the optimal planning layout (e.g. TES type, geometry, operation).

Construction of hot water tanks and pits require large investment; therefore, TES must be properly planned prior to construction to ensure the economic feasibility and efficient operation. Thus, numerical simulations found its place favorably permitting the planners to optimize the design and develop the operation. Hence, it is noteworthy to develop new models to appropriately and accurately simulate STES with feasible computation efforts.

LITERATURE REVIEW

Limits in numerical modeling of large-scale TES

Numerical modeling and simulation of large-scale TES systems unlocks the opportunity as an alternative to real experimental investigations. Yet, it is often held that numerical STES models tend to be costly in terms of simulation time. On a brighter note, numerical models pave the way to examine the impact of any player (e.g. dimensions, operation characteristic) on the STES performance without any actual economic cost related to construction.

To capture the insights, Chang et al. (Chang et al., 2017) developed and validated a CFD model perfectly tailored to investigate the impact of some characteristic parameters on pit TES efficiency. It was concluded that the efficiency drastically decreases as the slope angle becomes smaller. Additionally, a degradation in stratification degree was detected, which was attributable to the decrease in the PTES depth and, thus, less thermal efficiency.

CFD simulations certainly require enormous computation efforts and, currently, this is considered impractical. Thus, CFD simulations are ideally suited for specific tasks or short-term operations. To tackle this challenge, assumptions are made for a number of inputs (e.g. material properties) in simulations. Thereby, a positive notable reduction in the computation efforts is seen leading to the so-called "coarse models". In this context, a dynamic finite-element model was developed in Matlab/Simulink platform (Ochs, 2014). The model captures various TES shapes limited to circular cross-sections (i.e.

cylinder, cone) for underground hot water TES. Then, the model was further coupled to a finite difference model for the ground.

To reduce the models' complexity, (Sorknæs, 2018) developed a simulation method to simulate a pit TES coupled with a heat pump in a DH system. The simulation results were compared against measured data from Dronninglund pit TES for the year 2015. The simulated thermal losses were around 1741 MWh, whereas the measured thermal losses were around 1275 MWh. This discrepancy (approx. 35 %) highlights the inaccuracy of this method, which might deliver misleading conclusions during STES planning phase.

In coarse models, the "notable" reduction has a cost that often results into a shortcoming in the depiction of thermal hydraulic behavior in STES. Thus, coarse models do not accurately account for thermal losses, especially when the case comes to a more complicated modeling scheme (e.g. presence of groundwater flow).

Challenges in planning and construction of large-scale TES

The planning and construction of large-scale STES are often seen challenging in both technical and economic aspects (Dahash et al., 2019). This arises from the fact that such systems require great volumes to fulfill the seasonal tasks and, therefore, large space availability is needed.

Throughout the planning phase, some interesting questions start to arise in context of the construction type (e.g. partially or full buried) and geometry (e.g. tank, truncated cone or pyramid stump) and others while planning the optimal STES for a selected R-DH.

A substantial attention was paid to underline the players influencing the planning of a STES in (Dahash et al., 2019). The work emphasized that for a proper selection of a large-scale STES (design, geometry and construction type), a wide variety of inputs (hydro-geological factors, system characteristics, thermal losses, investment cost, etc.) are coherently evaluated to comprehend the impacts. Thereby, the decision-makers are informed which compromise between the technical performance and the economic investment is the optimal.

By means of numerical simulations, (Ochs et al., 2019) conducted a techno-economic analysis for large-scale TES. The study pointed out that a TES with 100 000 m^3 installed in LT-DH systems is more promising on both economic and technical aspects compared to its corresponding installed in HT-DH systems.

Contribution of this work

The authors present a numerical approach for modeling large-scale TES. Next, the model is validated against a valid finite-element, which is validated considering measured data from Dronninglund PTES in Denmark. Then, the work investigates the influence of tank shape on thermal performance and stratification. Next, the work techno-economically examines the influence of insulation thickness concerning tank performance and costs.

METHODOLOGY

Development of hot-water tank TES

The tank is developed using the partial stratified tank from the Modelica Buildings library (Wetter et al., 2013). The model is divided into a number (n) of segments in which each segment has a uniform temperature (T_i). Besides, the developed model allows more than a single incoming/outgoing stream of water. Therefore, multiple inlet and outlets are allowable.
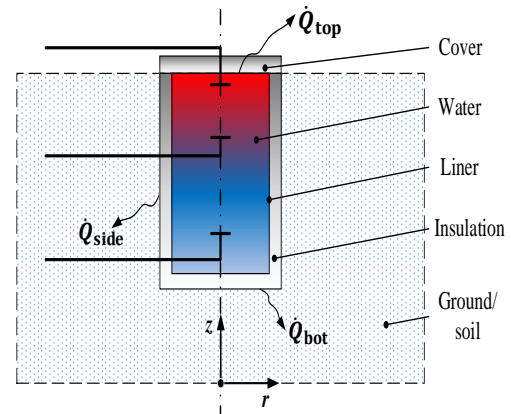

Figure 1: A 2-D representation of buried tank with 3 injection/extraction diffusers.

In the partial tank model, the major modification takes place in the enhanced thermal conductivity. Throughout TES storage and idle modes, a buoyancy-driven heat flow is dominating. This arises since water has a temperature-dependent density. Hence, a natural convection is consequently induced by buoyancy resulting into a water recirculation between the hot and cold regions close to the TES boundaries. Due to the high losses through the top of TES, a temperature drop might be observed at the very top of the storage near to upper surface area. This drop might form an undesired phenomenon known as "inverse thermocline" in the simulated stratification profile.

In order to tackle this shortcoming, the water heat conductive term is substituted with another term to enhance the thermal conductivity of water and, consequently, to eliminate inverse thermocline (Dahash et al., 2019). Accordingly:

$$A_i \nabla \cdot (\lambda_w \nabla T_i) = \begin{cases} A_i \nabla \cdot (\lambda_w \nabla T_i), & \dot{V}_w \neq 0 \\ A_i \nabla \cdot (\lambda_{w,enh} \nabla T_i), & \dot{V}_w = 0 \ and \ \dfrac{\partial T_i}{\partial z_i} < 0 \end{cases} \quad (1)$$

Where the enhanced thermal conductivity is theoretically originated from Nusselt and Rayleigh numbers and modified following the given application

(large-scale TES). Thus, to account for the influence of natural convection driven by buoyancy:

$$\lambda_{w,enh} = \lambda_w \cdot Nu \qquad (2)$$

Where Nusselt number requires two constants C and k that are usually experimentally determined. Accordingly, it can be stated:

$$Nu = C \cdot Ra^k \qquad (3)$$

$$Ra = \frac{g\beta \cdot \Delta T \cdot z^3}{\nu\alpha} \qquad (4)$$

g stands for the gravitational acceleration. Whereas β, ν and α represent the thermal expansion, kinematic viscosity and thermal diffusivity of water, respectively. Further, ΔT accounts for the temperature difference between the segments along the characteristic length (z) due to the difference in the vertical thermal conductivity imposed by natural convection. Consequently, the enhanced thermal conductivity obeys the following function:

$$\lambda_{w,enh} = C \cdot \left(\frac{\partial T}{\partial z}\right)^k \qquad (5)$$

Where C denotes a constant that brings different dimensional parameters (e.g. volume, height) together with thermo-physical properties (e.g. density, specific heat capacity, thermal expansion coefficient). Whereas the exponent k is usually experimentally determined and accordingly tuned depending on the application, storage medium and geometry (e.g. cylindrical or pit); however, $k = 0.5$ was confirmed to be the most applicable value to the investigated case.

Development of ground/soil model

This model is developed to predict the thermal interaction between the buried tank and the surrounding soil with a focus on long-term operations. It is established in a finite-difference fashion with a discretization in both radial and axial directions, so the ground's axial and radial temperatures are depicted. Consequently, the model consists of different nodes in both directions forming an adjustable mesh. Figure 2 illustrates the temperature field with the nodal network in axial and radial directions.

The gird is divided into (n_{rad}) and (n_{ax}) nodes in radial and axial directions, respectively. Each cell has two radii; one is inner and the other is outer. As thermal properties, the model involves the thermal diffusivity of the soil to fulfill the heat equation as follows:

$$
\begin{aligned}
\frac{\partial T_g(r,z,t)}{\partial t} = {} & \alpha \frac{\partial^2 T_g(r,z,t)}{\partial r^2} \\
& + \alpha \frac{1}{r} \frac{\partial T_g(r,z,t)}{\partial r} \\
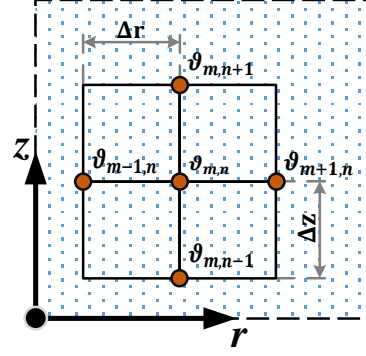& + \alpha \frac{\partial^2 T_g(r,z,t)}{\partial z^2}
\end{aligned} \qquad (6)
$$

Figure 2: Nodal network for the soil model.

Operation scenarios and boundary conditions

This work aims to develop buried tank models that are reliable and computationally fast enough to give insights into the STES planning. Thus, it is advantageous to eliminate system simulations (e.g. solar thermal collectors, heat pumps pipelines, customers) in order to avoid costly simulations in terms of simulation time and computation efforts. Still, DH operation profiles (i.e. temperature and flowrates) are crucial for the TES operation (i.e. charging/discharging modes). Thus, a simplified DH temperature profile is introduced in the model. The DH supply temperature is set to 90 °C and the return temperature is given as 60 °C. Figure 3 and Figure 4 show the simplified periodic operating conditions for a TES.
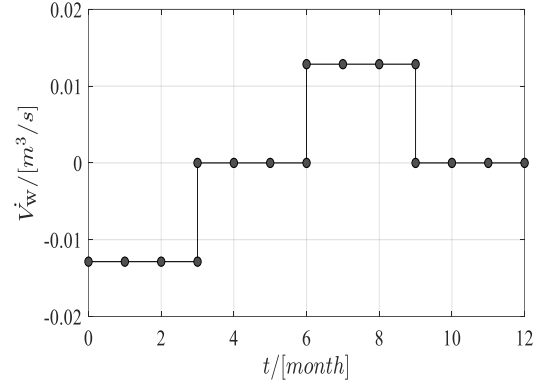

Figure 3: Water volumetric flowrate as a periodic function of the time for a tank with a volume of 100 000 m³.
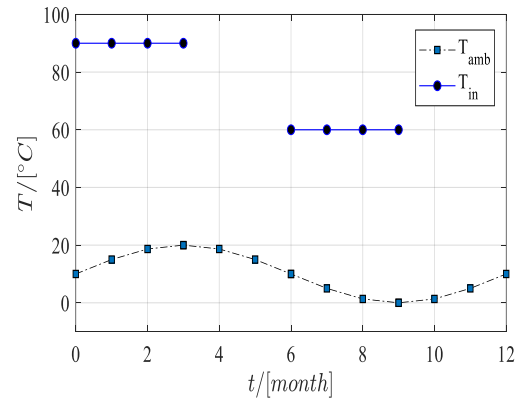

Figure 4: Flow temperature as a periodic function of the time and ambient temperature as a sinus function with an average of 10°C.

Performance indicators

In this work, TES energy capacity efficiency is used to indicate the tank thermal performance and it is given as below:

$$\eta_{\text{TES}} = 1 - \frac{Q_{\text{loss}}}{Q_{\text{TES}}} \qquad (7)$$

The importance of such a definition is the correlation between the annual thermal losses to the maximum theoretical storage capacity. In this regard, the storage losses depend on the operation scenario and boundary conditions and are determined by dynamic simulations. The storage capacity is a function of the TES volume and the maximum and minimum temperature:

$$Q_{\text{TES}} = V \cdot \rho \cdot c_p \cdot (T_{\text{max}} - T_{\text{min}}) \qquad (8)$$

Thermal stratification is a central element in TES performance as it influences the water temperatures inside the tank. Stratification depends on the tanks shape and aspect ratios. In this context, it is crucial to examine the influence of different aspect ratios on the stratification quality and, thus, two stratification measures are used in this work. One measure is the stratification number, Str(t), and obeys the following:

$$Str(t) = \frac{\overline{(\partial T/\partial z)}_{\text{t}}}{\overline{(\partial T/\partial z)}_{\text{max}}} \qquad (9)$$

Where:

$$\overline{(\partial T/\partial z)}_{\text{t}} = \frac{1}{n-1}\left[\sum_{i=1}^{n-1}\frac{T_{i+1} - T_i}{\Delta z}\right] \qquad (10)$$

$$\overline{(\partial T/\partial z)}_{\text{max}} = \frac{T_{\text{max}} - T_{\text{in}}}{(n-1)\cdot \Delta z} \qquad (11)$$

T_{max} represents the maximum temperature realized in the entire TES operation, whilst the minimum temperature is given by the inlet temperature. Further, Δz expresses the height between the adjacent segments at which temperatures are measured.

Whereas the second measure is the stratification efficiency, which is based on the MIX number shown below:

$$\eta_{\text{Str}} = 1 - \text{MIX} \qquad (12)$$

$$\text{MIX} = \frac{M_E^{\text{stratified}} - M_E^{\text{exp}}}{M_E^{\text{stratified}} - M_E^{\text{fully-mixed}}} \qquad (13)$$

Thus:

$$\eta_{\text{Str}} = \frac{M_E^{\text{exp}} - M_E^{\text{fully-mixed}}}{M_E^{\text{stratified}} - M_E^{\text{fully-mixed}}} \qquad (14)$$

This measure defines the stratification quality as it compares the moment of energy for the investigated tank compared to the perfectly-stratified and fully-mixed tanks. Accordingly, perfectly-stratified TES is characterized by the largest value for M_E, whereas fully-mixed ones have the smallest value of M_E and an experimentally TES system has a value in between. the moment of energy obeys the following expression:

$$M_E = \sum_{i=1}^{n} z_i \cdot Q_i = \sum_{i=1}^{n} z_i \cdot (\rho V_i) \cdot c_p \cdot T_i \qquad (15)$$

More information about these measures can be found in (Dahash et al., 2019) and (Haller et al., 2009).

In order to carry out a techno-economic analysis, it is important to use a measure that can reflect the influence of each insulation thickness on both performance and capital cost. Thus, this work suggests the levelized cost of storage (LCOS) as follows:

$$\text{LCOS} = \frac{C_{\text{fix}} + C_{\text{O\&M}}}{Q_{\text{dis}}} \qquad (16)$$

C_{fix} and $C_{\text{O\&M}}$ represent the annual fixed payments and operation maintenance costs, respectively. The annual fixed costs are computed via the tank total investment cost and the annuity factor, whereas the operation costs (e.g. maintenance) is estimated as 10 % of the annual fixed payments. Thus:

$$C_{\text{fix}} = C_{\text{inv}} \cdot ANF_{\text{n},i} \qquad (17)$$

$$C_{\text{op}} = 10\,\% \cdot C_{\text{fix}} \qquad (18)$$

$$ANF_{\text{n},i} = \frac{(1+i)^{\text{n}} \cdot i}{(1+i)^{\text{n}} - 1} \qquad (19)$$

The capital cost is estimated using the cost provided in (Ochs et al., 2019) for the different construction types and geometries. Yet, this work narrows the investigation down to the fully-buried tank with a volume of 100 000 m³ equipped with a floating cover as reported in Table 1. Assuming a service lifetime of n = 50 years and a discount rate of i = 3 %, then, ANF = 3.9 %.

Table 1: Specific costs for the tank construction (simplified)

Contribution	(Specific) Costs	Remark
Excavation	20 €/m³	Partly wet
Diaphragm wall	550 €/m²	50 m deep
Cut-off wall	50 €/m²	For groundwater in 5 m distance
Bottom insulation	100 €/m³	Pressure resistant
Wall Insulation	375 €/m³	Insulation cost
	100 €/m²	Installation
Liner	150 €/m²	Stainless steel
Floating cover	200 €/m²	With 50 cm insulation
Plant construction	40,000 €	Independent of construction
Site facilities	50,000 €	Fixed

RESULTS AND DISCUSSION

Validation of Modelica TES model

To gain trust in the developed tank model, it is crucial to compare the model outcomes against measured data. Herein, the tank model developed in Modelica is

cross-validated against a finite-element model developed in COMSOL Multiphysics, which was already validated against Dronninglund pit TES in Denmark (Dahash et al., 2020). Subsequently, the COMSOL model is the benchmark in this study. It is worthy to mention that COMSOL model considers the heat transfer in the solid domain (i.e. soil) as physics-based, whereas the fluid domain (i.e. TES) is developed as equation-based to simulate the multi-physical aspects (heat transfer, fluid flow) in order to avoid lengthy CFD-simulations for such large-scale TES (Dahash et al., 2020). The proposed buoyancy model is originated from numerical and experimental investigations and prior reports.

For the validation, a tank with a volume of 2 000 000 m^3 and a height of 50 m is used as the validation case study. Moreover, it is presumed the tank has a lid with $U_{top} = 0.15$ W/(m^2.K) and insulation for the bottom and mantle; $U_{side} = U_{bot} = 0.3$ W/(m^2.K).

Figure 5 demonstrates a notable matching for the top, middle and bottom in the temperature profiles between both simulated tanks in the different tools. Yet, not only shall the temperature profiles be matching but also the thermal losses. Therefore, Table 2 reports the breakdown of thermal losses for and provides the relative error in the total thermal losses over the five years of investigation.

Simulation-based optimization

To run the simulations, Figure 4 is used to represent the temperature profile in the R-DH system. Accordingly, a series of simulations is presumed to start on May 1st of each simulation year during which the charging phase starts and, then, over a course of three months the storage is injected with renewable-based heat carried by hot water. This phase is followed by a 3-months storage phase. Next, the discharging phase takes place followed by 3 months of idle phase. The simulation timespan is set up for a 10-years operation permitting the STES system to reach its operating capacity and to allow the ground to pass the preheating. A single-day simulation time step is utilized in the numerical model. However, shorter time steps did not provide remarkable deviation in results.
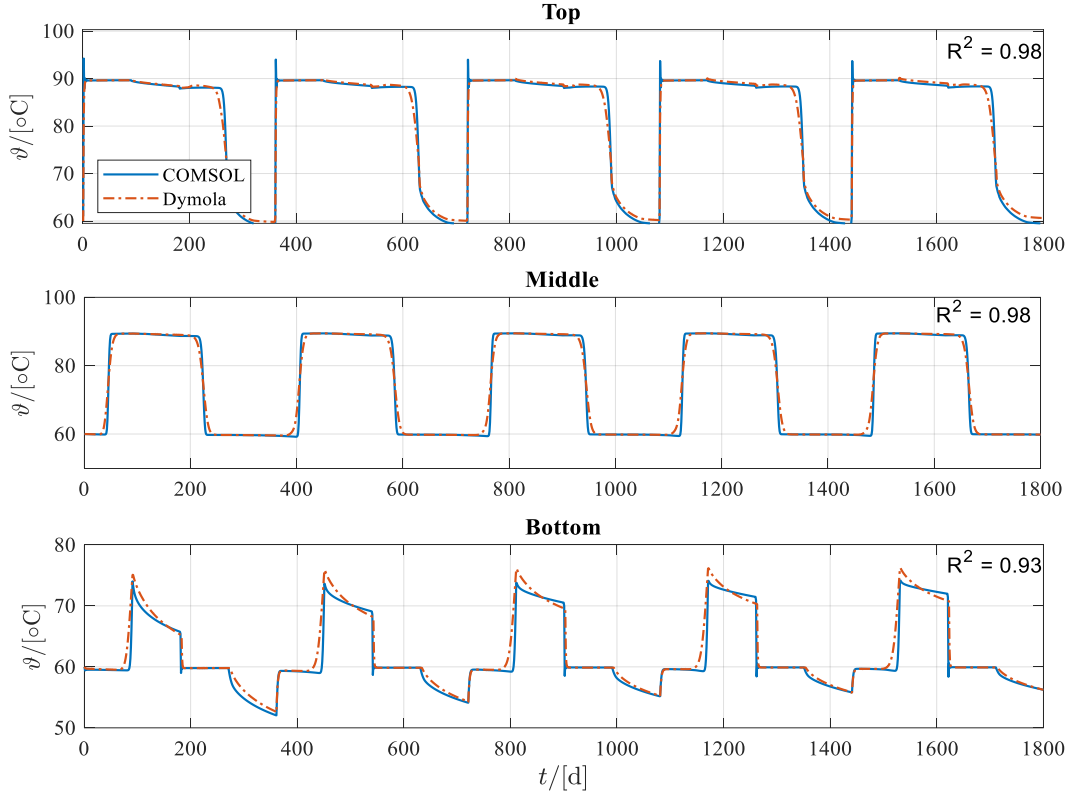

Figure 5: Temperature development at the 5th year for the cross-validation between COMSOL and Dymola.

Table 2: Breakdown of the annual thermal losses for the cross-validation of the tank model.

Year	Dymola				COMSOL			
	Q_{top}	Q_{side} [MWh]	Q_{bot}	Q_{loss}	Q_{top}	Q_{side} [MWh]	Q_{bot}	Q_{loss}
1	3432	2785	2149	8365	3428	2785	2148	8361
2	3364	2037	1550	6952	3364	2035	1549	6948
3	3368	1815	1272	6455	3366	1814	1271	6451
4	3368	1702	1116	6186	3368	1699	1115	6181
5	3385	1631	1016	6032	3384	1628	1013	6026

Influence of tank shape on TES performance

In order to demonstrate the role of tank shape when planning a large-scale TES, it is crucial to highlight the role of aspect ratio, which is a quotient of TES height to TES diameter. Thus, a 100 000 m^3 tank is simulated with $U_{top} = 0.15$ W/(m^2.K) and $U_{side} = U_{bot} = 0.3$ W/(m^2.K).

Figure 6 documents the total thermal losses for a variety of tank shapes as the aspect ratio increases. It inevitably demonstrates that the thermal losses decline as the surface area-to-volume ratio (SA/V) decreases. This is also recognized as the aspect ratio reaches a value of (AR = 1). Then, the losses start to increase as a consequence to the increase in SA/V, which is attributable to the role played by the tank's surface area.

Accordingly, the SA/V is an important consideration in a large-scale seasonal TES since it has a direct impact on the external losses from the TES. Therefore, it is recommended to maintain a small SA/V ratio. Besides, the most promising aspect ratio is (AR = 1) since it effectively reduces the total thermal losses.

Together with space availability, it is crucial to pinpoint that some hydro- geological conditions emerge as barriers from realizing the aimed aspect ratio and, subsequently, unfavorable aspect ratios were applied for several large-scale TES worldwide.
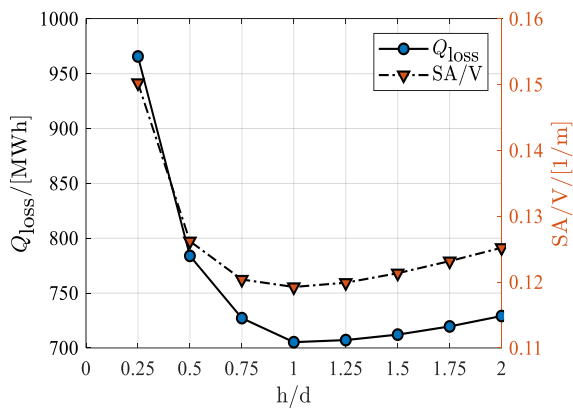

Figure 6: Thermal losses at the end of the 5th year for a tank with 100 000 m^3.

Influence of tank shape on thermal stratification

A key player for a good stratification is the tank shape because an improper TES geometry might enhance the mixing leading to stratification decay and, thus, exergetic losses. This section elaborates the tank shape influence on the stratification quality. Given some economic limits, the maximum feasible depth for a buried tank is limited to 50 m; consequently, this excludes shapes with (AR > 1) in this investigation since the excavation below 50 me is not feasible.

Figure 7 reveals the development of the stratification number and stratification efficiency for a 100 000 m^3 tank with 4 aspect ratios. This evaluation is applied over the 5th operational year. In this context, 4 TES operative phases are clearly recognized that are: charging, standby, discharging and idle, which correspond to A, B, C and D, respectively.

Figure 7 depicts that TES stratification quality tends to decrease over the 1st half of charging phase and, then, it increases indicating a good stratification quality. This phenomenon can be justified that during the 1st half more than half of TES volume is filled with water at 60°C (initial temperature) and, simultaneously, 90°C hot water is injected from the top diffuser. Whereas in the 2nd half, more than half of TES volume is filled with hot water and, meanwhile, charging carries on.

In the region (B), TES undergoes a standby mode in which no incoming/outgoing flowrates and, therefore, stratification maintains a good quality with a slight decay attributed to the thermal losses from TES envelope. Besides, TES experiences a buoyancy-driven heat flow over the standby mode and, subsequently, mixing is enhanced. Over this period, TES with aspect ratio of (AR = 1) exhibits a notable stratification quality compared to other aspect ratios.

Whereas throughout the region (C), TES discharges the stored energy to R-DH network and is injected with 60°C water from the return line. Therefore, the stratification quality suddenly experiences a decline due to the extraction of hot water from the upper diffuser and, simultaneously, injection of water with water at 60°C from the bottom diffuser. Then, the stratification gradually builds up and improves leading to better quality by the end of this phase.

Period (D) is similar to period (B) whereby conductive heat transfer is dominating with no incoming and outgoing flowrates. Therefore, this period is characterized with initial mixing that is promptly counterbalanced by equation (5) in order to avoid misleading results by inverse thermocline. Yet, the good level of stratification is also attributed to thermal losses that bring the tank to lower temperatures than that of DH return temperature.

Having considered stratification measures, a tank shape with (AR = 1) exhibits the premium stratification quality among other options. It also has less surface area and, consequently, less thermal losses. Thereby, this tank has higher quality of energy delivered to DH in terms of temperature.

Techno-economic analysis for insulation thickness

Herein, the insulation thickness investigated is subjected to the following, $X_{ins} = [0\ 10\ 25\ 50\ 75\ 100\ 120\ 160\ 200\ 220\ 240\ 260]$ mm. The increase in the insulation thickness reduces the annual thermal losses leading to ultimate increase in the performance. Figure 8 depicts an increase of around 11 % in the tank performance if the option with 260 mm insulation thickness is chosen over the case with no insulation.
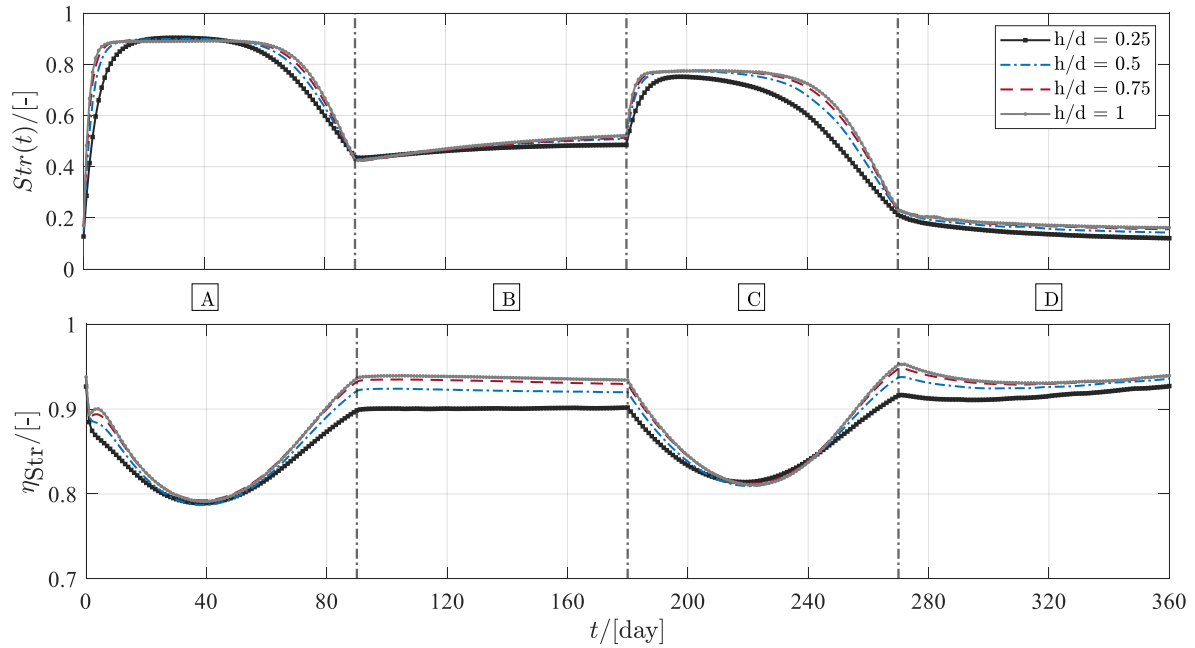
Figure 7: Stratification number and stratification efficinecy development over the 5th year for a a 100 000 m³ buried tank.

Inevitably, this increase has an impact on the energy delivered by the tank and, thereby, the yearly amount of discharged heat to the heating grid also increases to appx. 300 MWh as shown in Figure 9. This increase accounts for around 11 %.
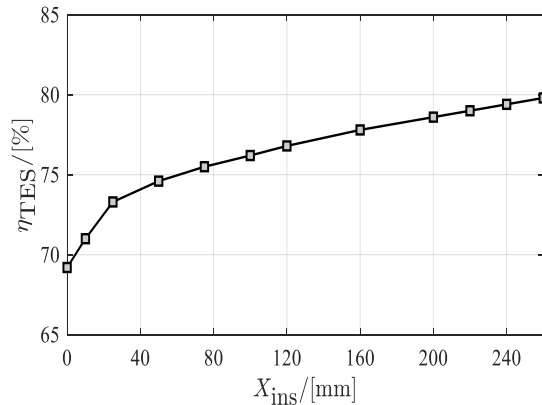

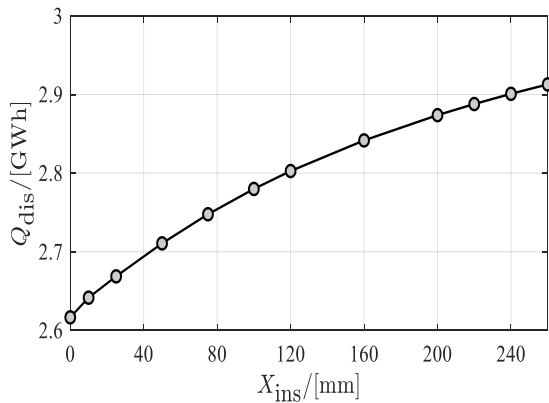*Figure 8: Tank efficinecy at the end of the 5th year for different insulation thicknesses.*

Figure 9: Tank discharged heat at the end of the 5th year for different inuslation thicknesses.

Concerning the influence of this increase on the LCOS, Figure 10 illustrates the trend for the different thickness scenarios. It is remarkably seen that despite the increase in the yearly amount of heat discharged, there is a notable increase in the LCOS and, accordingly, this draws attention that there is a relative increase also in the specific capital cost.

Figure 10 depicts that approx. 10 €/MWh is added when insulation with 260 mm is installed for the side wall and the bottom and the corresponding profit can be computed by assuming a heat selling price of 55 €/MWh with an additional yearly amount of 300 MWh discharged energy, then, an increase of 16500 €/a, which accounts for additional 11 % more profit compared to the non-insulated case. However, this also triggers the capital cost to increase by approx. 19 % if the well-insulated case is chosen and this corresponds to approx. 1,622,010 € if the well-insulated case is chosen over the uninsulated one.
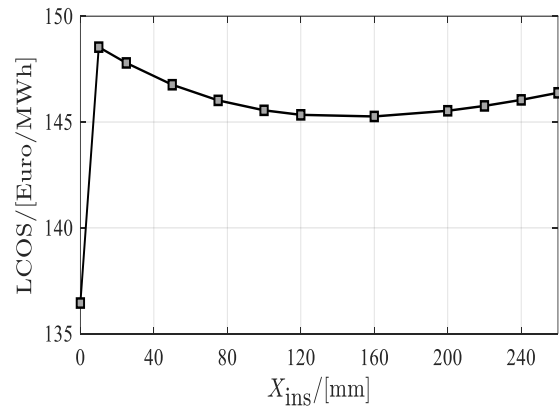

Figure 10: Tank LCOS for different insulation thicknesses.

Yet, it is important to mention that these results are applicable only for the case investigated under the given boundary conditions. In other words, a sensitivity analysis for each single parameter is necessary in order to evaluate the parameter's influence on the techno-economic analysis leading to well-established planning guidelines.

CONCLUSION

As the ultimate goal strives for a 100 % renewable heat supply in the DH domain, it is crucial to equip those systems with large-scale TES volumes. Yet, it is important to plan these systems properly and feasibly in order to ensure the perfectly tailored cost-effective option for each given R-DH. Otherwise, the TES performance would be below expectations with enormous capital expenditure. Therefore, numerical simulations emerge as an alternative to real-world experiments. Thereby, it notably reduces the costs with drastic increase in the in-depth knowledge leading to proper planning of large-scale TES.

This work investigated the numerical modeling of large-scale TES in an equation-based object-oriented programming language (i.e. Modelica). Later, the model was cross-validated against a valid numerical model that was validated against measured data from an existing real-world large-scale TES. The results revealed a remarkable agreement between the models.

Then, simulation-based optimizations ran to examine the impact of tank shape on tank thermal performance and thermal stratification. The study depicted that tanks with (AR = 1) tend to have the optimal performance and stratification compared to other aspect ratios. Whereas the aspect ratio (AR = 0.25) delivered the worst stratification and this was attributed to the tank height and the large cover area leading to higher amount of annual thermal losses.

To techno-economically evaluate the influence of insulation thickness on STES performance, the LCOS was calculated for the list of thicknesses chosen in this work. The highest possible thickness of 260 mm depicted a notable increase in STES performance and, accordingly, an increase in the yearly discharged heat. However, this thickness led to a significant increase in the capital cost.

It is important to highlight the model developed has a downside, which is the limitation to tank shapes. In other words, the model is not capable to represent sloped-walls TES (e.g. truncated cone) and this challenge will be tackled in future work.

ACKNOWLEDGEMENT

REFERENCES

Chang et al. (2017). Influences of the key characteristic parameters on the thermal performance of a water pit seasonal thermal storage. *Energy Procedia, 142*, 495-500. doi:10.1016/j.egypro.2017.12.077

Dahash et al. (2019). Advances in seasonal thermal energy storage for solar district heating applications: A critical review on large-scale hot-water tank and pit thermal energy storage systems. *Applied Energy, 239*, 296-315. doi:10.1016/j.apenergy.2019.01.189.

Dahash et al. (2019). Numerical analysis and evaluation of large-scale hot water tanks and pits in district heating systems. *Building Simulation 2019 Conference*, *29*, pp. 1692-1699. Rome (Italy), 02-04 September 2019. doi:doi.org/10.26868/25222708.2019.210566

Dahash et al. (2020). Toward Efficient Numerical Modeling and Analysis of Large-Scale Thermal Energy Storage for Renewable District Heating Systems (Submitted manuscript). *Applied Energy*.

Haller et al. (2009). Methods to determine stratification efficiency of thermal energy storage processes – Review and theoretical comparison. *Solar Energy, 83*(10), 1847-1860. doi:10.1016/j.solener.2009.06.019.

Ochs et al. (2019). Techno-economic planning and construction of cost-effective large-scale hot water thermal energy storage for Renewable District heating systems. *Renewable Energy, 150*, 1165-1177. doi:doi.org/10.1016/j.renene.2019.11.017.

Ochs, F. (2014). Large-Scale Thermal Energy Stores in District Heating Systems – Simulation Based Optimization. *Proceedings of EuroSun 2014: International Conference on Solar Energy and Buildings.* Aix-les-Bains (France), 16-19 September 2014.

Sorknæs, P. (2018). Simulation method for a pit seasonal thermal energy storage system with a heat pump in a district heating system. *Energy, 152*, 533-538. doi:doi.org/10.1016/j.energy.2018.03.152.

Wetter et al. (2013). Modelica Buildings library. *Journal of Building Performance Simulation , 7*(4), 253-270. doi:doi.org/10.1080/19401493.2013.765506